

Real Time Discrete Optimized Adaptive Control for Ionic Polymer Metal Composites

KYRIAKOS TSIKMAKIS, VASILEIOS DELIMARAS, ARGYRIOS T. HATZOPOULOS,
MARIA S. PAPADOPOULOU

Department of Information and Electronic Engineering,
International Hellenic University,
Sindos, 57400,
GREECE

Abstract: - This paper describes a proposed method for optimizing the parameters of a Model Reference Adaptive Control (MRAC) system. The MRAC system uses a reference model to control a plant with unknown dynamics and continuously updates its parameters to improve control accuracy. The system requires an adjustment of parameter γ , which participates in the feedback of the system but cannot be adjusted in real time through trial and error. The proposed method uses optimization techniques to adjust the γ parameters in real time, specifically at the start of the control process, when the maximum deviation of the plant from the reference model is observed. The optimization technique varies the parameters and seeks the best solution to quickly reduce the error. Once the optimal solution is found, the optimization is turned off, allowing the MRAC to continue efficiently reducing the error. In the case of sudden changes in the error due to endogenous or exogenous factors, optimization is activated again to redefine the γ parameters. The magnitude of the change depends on the rate of error changes. The response of the IPMC was measured and compared against a reference signal using three different control techniques MRAC, Model Reference Adaptive Control (MRAC), MRAC-Taguchi, and MRAC-Taguchi-DCT, and the results show that the last penalizes frequencies beyond the fundamental frequency through the cost function, resulting in negligible harmonic distortion.

Key-Words: - IPMC, Taguchi Optimization, Model Reference Adaptive Control, DCT.

Received: September 27, 2022. Revised: January 4, 2023. Accepted: February 7, 2023. Published: March 7, 2023.

1 Introduction

An Ionic Polymer Metal Composite (IPMC), is a type of smart material that is made by sandwiching an ion-exchange membrane between two metal electrodes. The ion-exchange membrane is composed of a hydrated polymer, typically Nafion, which is capable of transporting ions. When an electric potential is applied across the metal electrodes, it creates an electric field within the ion-exchange membrane, causing the ions to move and create an actuation force. On the other hand, IPMC sensors use IPMC to detect changes in mechanical stress, pressure, or other physical parameters [1-2].

IPMCs have several interesting properties, such as fast response time, high sensitivity, low driving voltage, and excellent durability. These properties have made IPMCs attractive for a wide range of applications, including artificial muscles, MEMS, actuators, grippers, sensors, and energy harvesting, owing to their fast response time, high sensitivity, low driving voltage, and excellent durability [3-5].

IPMCs can be modeled and controlled using several different techniques, including electrical and

mechanical models. These models can be used to design and optimize IPMC systems for various applications, as well as to predict the behavior of IPMCs under different operating conditions [6-8].

All these important manufacturing factors influence the dynamic response of the material when functioning as an actuator, making it challenging to find an analytical model of the system.

Developing a control strategy is a viable option for ensuring a certain dynamic reaction from the IPMC. Various authors have worked on the design of control techniques for IPMC materials with various goals [10].

PID, MRAC, and LQR control are among the main control algorithms used for controlling ionic polymer composite (IPMC) actuators. However, there are some differences in their effectiveness and complexity. PID control is the most common and simplest control algorithm used in the IPMC actuators. It is a linear control algorithm that uses a proportional term, integral term, and derivative term to control the position of the IPMC actuator. The PID controller is simple to implement and can be

easily adjusted to satisfy the requirements of the system. However, its linearity makes it less effective in controlling nonlinear systems, such as IPMC actuators [10]. MRAC control is a nonlinear control algorithm that uses a model reference adaptive control approach. It adjusts its control strategy in real-time to accommodate changes in the system and improve its performance. This makes MRAC more effective than PID control in controlling nonlinear systems [11]. However, MRAC requires more computational resources and is more complex to implement than PID control. LQR control is a linear quadratic control algorithm that optimizes the performance of a control system based on a mathematical model of the system [12]. LQR control uses a weighting matrix to balance the trade-off between the control effort and control performance. LQR control is more effective than PID control [13] and MRAC control in controlling IPMC actuators because it takes into account the nonlinearity of the system. However, the LQR control is also more complex and computationally intensive than the other two algorithms.

The choice of control algorithm for IPMC actuators depends on the requirements of the system and available computational resources. PID control is the simplest and easiest to implement, whereas LQR control is the most effective but also the most complex, and it is very difficult to implement them in microcontrollers. The MRAC control is a good compromise between the two, providing good performance and ease of implementation.

The purpose of this control is to ensure the same reaction, even if the dynamic behavior of the beam changes over time. The proposed control technique is based on a reference model-adaptive control MRAC scheme. This type of strategy adjusts its control rule to account for the fact that the actuator parameters change over time. The control technique involves compelling the entire system to conform to a user-defined model reference system behavior, even though the IPMC actuator response varies over time.

Several authors have attempted to reduce the effect of an actuator's dynamic drifts on the final closed-loop response by employing robustness strategies [14-15]. The MRAC control used in our study was virtually insensitive to model dynamic changes.

If γ remains constant, then for various frequencies, the error takes longer to reach zero or can even cause the system to become unstable.

For different frequencies, we need to adjust γ -MRAC to avoid instability and increase the speed of adaptation. In addition, a discrete form of the

control system is necessary for applying optimization and analysis algorithms.

To improve the real-time system of adjustment at various frequencies, optimization using the Taguchi algorithm [16] and discrete cosine transform (DCT) analysis were performed [17].

Discrete cosine transform (DCT) is a type of mathematical transform that is widely used in digital signal processing, image compression, and audio compression. It converts a signal from its original time or spatial domain into a transformed domain, where the frequency components of the signal are represented by a series of coefficients.

DCT is a powerful tool for determining the frequencies present in a set of discrete data points. DCT provides a clear representation of the frequency content of the data by transforming the data into a set of cosine functions with different frequencies.

In this study, an improved MRAC system for the fast and stable control of an IPMC strip was implemented for use in embedded systems. One potential use of our control with an IPMC strip is to control the motion of a robotic fish or robotic arm that uses artificial muscles made of IPMC materials. Using the proposed controller, the system could adapt its control parameters faster based on the changing dynamics of the IPMC actuators, allowing for more precise and robust control.

2 Subject & Methods

2.1 IPMC Model and Setup

The transfer function model identification of an ionic polymer-metal composite (IPMC) involves measuring the voltage response of the IPMC to a known input signal, such as a step function, sweep wave, or mixed signal, and then using mathematical techniques to fit a transfer function model to the measured response. The transfer function model represents the relationship between the input signal and output response and can be used to predict the performance of the IPMC under different conditions.

The transfer function obtained from the model identification is of 4th order, but to be used in the MRAC system, this means needed to be easily implementable in discrete-time systems such as microcontrollers, the 2nd order reduced version was preferred, which is shown below in the z-domain.

$$H(z) = \frac{0.5317z - 0.5317}{z^2 + 1.99z - 0.9899} \quad (1)$$

Measuring the displacement of an ionic polymer metal composite (IPMC) material using a laser is a common technique used in the research and development of these materials.

In general, the displacement of an IPMC can be measured using a laser-displacement sensor. This type of sensor uses a laser to measure the distance between the sensor and target surface. The displacement can be calculated by reflecting the laser off the surface of the IPMC and measuring the time it takes for the light to return to the sensor. Displacement can be measured in real time as the IPMC deforms and changes its shape.

It is important to note that the accuracy of displacement measurement can be influenced by several factors, including the resolution of the laser sensor, reflectivity of the surface of the IPMC, and stability of the laser beam. To ensure accurate measurements, it may be necessary to use high-resolution laser sensors and calibrate the sensors before use.

The experimental setup is shown in Fig.1.

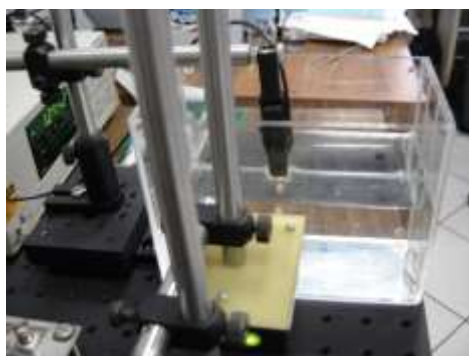


Fig. 1: The experimental setup.

2.1 MRAC Analysis

Model Reference Adaptive Control (MRAC) is a technique that uses a reference model to control a plant with unknown dynamics. The reference model represents the desired behavior of the plant, and the control algorithm adjusts the control input to ensure that the plant follows the reference model as closely as possible. In the MRAC, the controller continuously updates its parameters to improve the accuracy of the control process. This results in a more accurate control signal, even in the presence of changes in plant dynamics over time.

In a previous work [11], it was mentioned that γ , which participates in four points in the feedback of the system, can be adjusted by the user. However, this cannot occur in a real system, where the trial-and-error method is difficult to apply. In addition, the strain of the material and environmental conditions of the system operation are all factors

that lead to a change in the response of the IPMC. Thus, the IPMC should not receive a one-time constant value for the entire duration of system operation. Furthermore, the parameter is set for a specific operating frequency and needs to be set to a different value when the frequency is changed. This creates the need for an adjustment of γ in real time and for any changes that occur in the system. The error between the output of the plant and reference model is shown in Fig.2, when MRAC attempts to fit the response of the plant to the reference model for different frequencies and with the same value of γ .

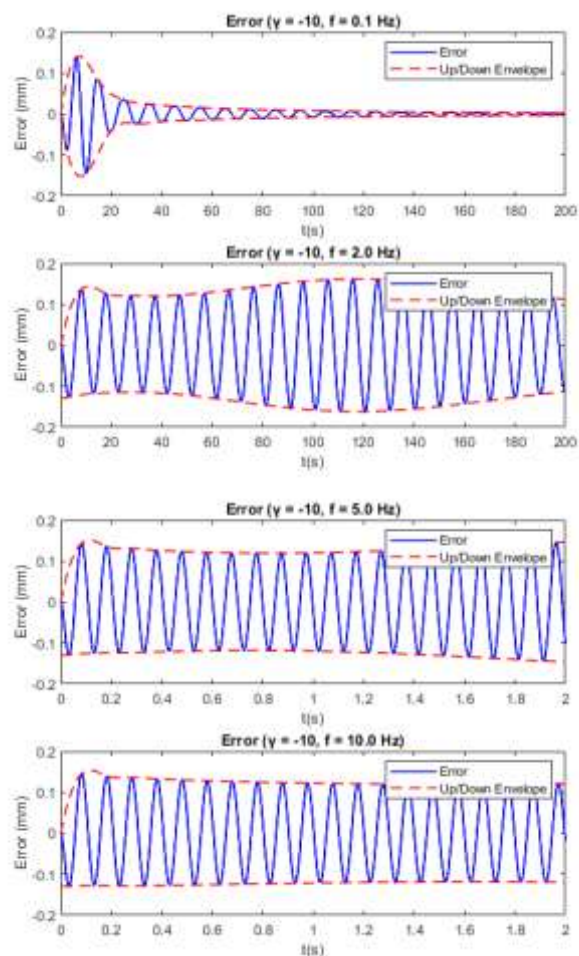


Fig. 2: Error between the output of the plant and the reference model for $\gamma = -10$ and various frequencies.

A value of $\gamma = -10$, it does not work properly for all frequencies. Even at a low frequency of 100 mHz, where the error approaches zero, the time required for the error to be considered negligible exceeds 30 s.

The error between the plant and reference model for $\gamma = -150$, is shown in Fig.3.

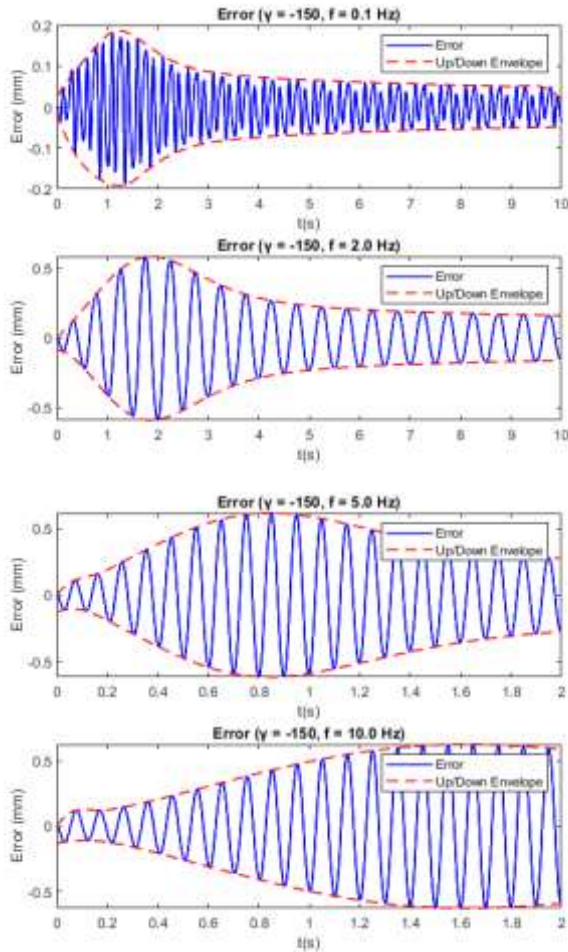


Fig. 3: Error between the output of the plant and the reference model for $\gamma = -150$ and various frequencies.

For frequencies of 100 mHz and 2 Hz, we observe that with this value of γ , the error decreases faster in contrast to frequencies of 5 Hz and 10 Hz, but still takes a long time to approach zero. In addition, when γ is high, MRAC works more aggressively on the system and with fast responses, which can also lead to vibrations and mechanical stress. Fast responses of the system are also seen in the 100 mHz error changes, where the error changes not only at the input frequency but also at higher frequencies. In Fig.4, the DFT spectrum of the error is shown for an operating frequency of 100 mHz input when γ has values -10 and -150, respectively.

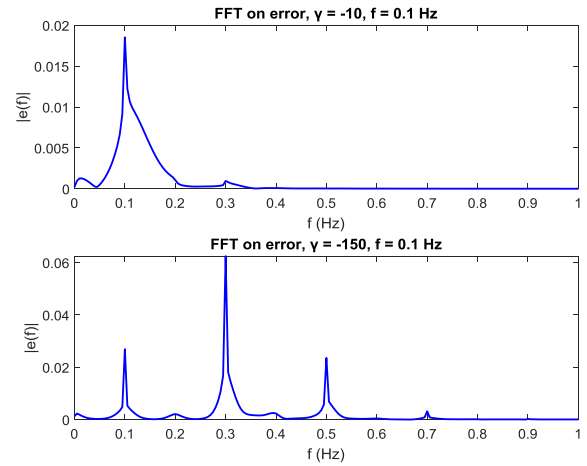


Fig. 4: DFT spectrum of the error for 100 mHz input for $\gamma = -10$ and $\gamma = -150$.

The system response produces harmonics owing to high γ values. This occurs when the MRAC attempts to adjust the plant input appropriately such that the plant's output matches that of the reference model. Fig.5 presents the output of the plant compared to the reference model for the above operating frequency and γ values.

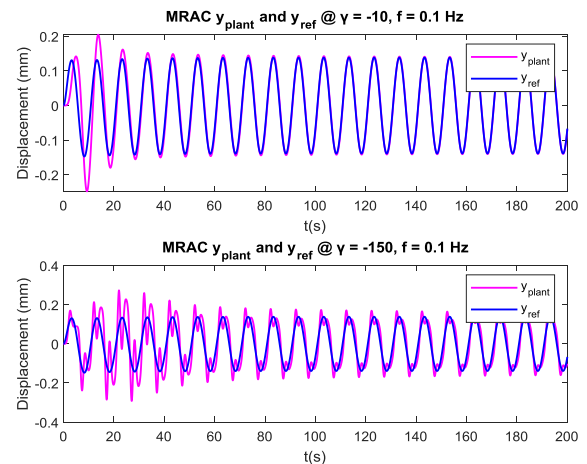


Fig. 5: The output of the plant has been compared to the reference model for 100 mHz input, $\gamma = -10$ and $\gamma = -150$ respectively.

It should be emphasized that parameter γ cannot have a fixed value and should be adjusted with the rest of the endogenous parameters of the system, but also with various exogenous factors that affect the system. Optimization of some parameters of a real-time controller is achieved with many iterations of the input before the controller starts working in real time for the system it is intended for. This occurs due to changes in the controller parameters cause the system output to diverge from the target. As a result, as the controller tries to return the error to zero, it becomes increasingly difficult to

do so as the parameters of the controller change. Owing to the aforementioned factors, the optimization of these parameters is not applied in real time.

On the one hand, this can cause strain on the plant; on the other hand, for every change in the parameters, the system must be shut down to re-adjust its parameters.

2.1 Improved MRAC using Taguchi Optimization

In the proposed method, optimization techniques are used and will act in real time during the system startup. The principle of operation is based on the fact that the MRAC requires some time to adjust the output of the plant with the reference model, and at the start of the control, the maximum deviation (error) of the plant from the reference model is observed. During this initial period, the proposed method was exploited to optimize the system parameters, specifically γ . Because optimization techniques and not the trial-and-error method will be used, it is easier in the four different feedbacks in which γ participates to optimize four different γ_i ($\gamma_1, \gamma_2, \gamma_3,$ and γ_4) instead of a common one to provide the maximum flexibility in the system to find a better solution, which will lead to a desired output.

At the initial time interval, where the maximum deviation occurs, that is, the maximum error, optimization techniques can vary the parameters and examine how quickly the error decreases or not. In addition, within this interval, the best solution for the parameter values that lead to a faster reduction in the error is sought. Once this solution is found, the optimization is turned off, and with the optimal parameter values, the MRAC is free to continue reducing the error further and more efficiently. The continuous operation of the optimization algorithm throughout the MRAC causes continuous deviations in the error-zeroing process and creates continuous oscillations in the system.

In the proposed technique, the optimization method starts dynamically and more aggressively to change the γ_i parameters within a short period of time. Over time, the effect of the optimization technique on the γ_i parameters decreased, leaving the normal operation of the MRAC free.

Any endogenous or exogenous factors can cause a sudden and significant change in error when the MRAC is operating in normal mode (where the error tends to be zero). Subsequently, the optimization is activated again to redefine the γ_i parameters. The optimization technique adjusts the values of the γ_i parameters. The magnitude of the

change depends on the rate of error changes e , from a predetermined number of samples n , according to the following relationship (2):

$$\gamma'_i = \gamma_i + \gamma_i \frac{\Delta e}{\Delta n} (1 - RP) \quad \text{for } i = 1, 2, 3, 4 \quad (2)$$

where γ'_i is the new value of the γ_i parameters and RP is an initial scaling factor of the γ_i parameters, where $RP < 1$.

In addition, during the process, the optimization technique reduces its effect on the variation of parameters γ_i . This is achieved by continuously increasing the coefficient RP ; thus, the new value of RP' is given by (3).

$$RP' = RP + (1 - RP) RP_{SF} \quad (3)$$

where RP_{SF} is a scaling factor of the RP factor and $RP_{SF} \leq 1$. As the coefficient RP approaches unity, the change in parameters γ_i will be smaller, until finally, no change occurs.

Taguchi optimization is an iterative optimization method based on orthogonal arrays developed by Taguchi [18]. Each row of the array is a combination of values of the parameters to be optimized. In each column of the array, the values of each parameter, which were defined in levels, were placed. Each level is a percentage change in the value of the parameter, from its initial value when the array was initialized.

For example, in Table 1, a Taguchi orthogonal array of four factors (in our case, the γ_i parameters) with three levels for each factor, named L9, is depicted.

Table 1. The Taguchi L9 orthogonal array of four factors.

Experiment Numbers	γ_1	γ_2	γ_3	γ_4
1	1	1	1	1
2	1	2	2	2
3	1	3	3	3
4	2	1	2	3
5	2	2	3	1
6	2	3	1	2
7	3	1	3	2
8	3	2	1	3
9	3	3	2	1

Initially, a value (even random) is defined for each factor that constitutes level 2, and the number 2 of each column in the array is replaced by these initial values.

Level 1 is a negative percentage change of central level 2, on the other hand, level 3 is a positive percentage change of central level 2. This is exactly the meaning of the *RP* coefficient, the percentage increase or decrease of each factor to create the three levels.

This array constitutes the design of experiments (DOE), that is, each row of the array is a combination of factor values to be tested and evaluated by a fitness function (or cost function, objective function, etc.). The array contains a subset of all possible combinations to run in a certain region to locate the value on which each factor must converge to achieve a better score in the fitness function.

The algorithm determines the effect of each variable on output. It identifies the value (level) of each factor that offers the best solution through the relationship expressing the signal-to-noise ratio or SN:

$$SN_i = 10 \log \left(\frac{\bar{y}_i^2}{s_i^2} \right) \quad (4)$$

where i is the experiment number (array row), \bar{y}_i is the mean value of the Cost Function, and s_i^2 is the variance. The average value \bar{y}_i is given by (5):

$$\bar{y}_i = \frac{1}{N_i} \sum_{u=1}^{N_i} y_{i,u} \quad (5)$$

where u is the number of trials, and $y_{i,u}$ is the value of the Cost Function for the given experiment i and trial u . Finally, N_i is the total number of trials in the experiment i .

The calculation of variance s_i^2 is given by (6):

$$s_i^2 = \frac{1}{N_i-1} \sum_{u=1}^{N_i} (y_{i,u} - \bar{y}_i)^2 \quad (6)$$

The Cost Function score is evaluated for each array combination. Either the score value should be increased (positive or negative) as much as possible, either to tend to zero. Therefore, the "minimum is better" and "maximum is better" cases are distinguished, depending on the problem. Thus, relation (4) is formulated as follows for the "minimum is better" case:

$$SN_i = -10 \log \left(\sum_{u=1}^{N_i} \frac{y_u^2}{N_i} \right) \quad (7)$$

and for the case "maximum is better":

$$SN_i = -10 \log \left(\frac{1}{N_i} \sum_{u=1}^{N_i} \frac{1}{y_u^2} \right) \quad (8)$$

The algorithm then calculates the mean value of SN for each factor and level according to equation (9):

$$SN_{f,L} = \frac{1}{L} \sum_{i=1}^R SN_{i,L} \quad (9)$$

where f is the number of the factor (column of the array), L is the number of the level and R is the total number of experiments (total number of rows of the array).

Table 2 contains the mean value $SN_{f,L}$ for each factor and level.

Table 2. The mean value $SN_{f,L}$ for each factor and level.

Level	γ_1	γ_2	γ_3	γ_4
1	$SN_{1,1}$	$SN_{2,1}$	$SN_{3,1}$	$SN_{4,1}$
2	$SN_{1,2}$	$SN_{2,2}$	$SN_{3,2}$	$SN_{4,2}$
3	$SN_{1,3}$	$SN_{2,3}$	$SN_{3,3}$	$SN_{4,3}$
ΔSN_f	ΔSN_1	ΔSN_2	ΔSN_3	ΔSN_4
Rank				

For each factor, the range of variation of $SN_{f,L}$, is calculated, with the relation (10):

$$\Delta SN_f = \max(SN_{f,L}) - \min(SN_{f,L}) \quad (10)$$

and is filled in on a new line of Table 2.

The greater the range ΔSN_f in a parameter, the greater the effect of the variable on the system and, consequently, on the optimization process.

This occurs because the same percentage change in a parameter (signal) causes a greater effect on the output of the system and consequently on the Cost Function.

In the "Rank" line of Table 2, the position of the most important parameter is filled. All ΔSN_f are sorted in descending order, the one that will be first, and therefore the largest, will get the number 1, and the rest are filled in the same way.

The levels of each parameter for the optimization process are chosen, where $SN_{f,L}$ is the maximum or the minimum, depending on the "maximum is better" or "minimum is better" case. This is because the values of these levels have the maximum effect on the Cost Function.

The values of the levels of each factor that offer a better score in the Cost Function are placed as central (level 2) and the process is repeated again from the beginning, until the goals set are achieved.

2.2 Improved MRAC using Taguchi-DCT Optimization

The Taguchi optimization chooses the appropriate γ_i , but it does not consider the spectral content of the response, resulting in an optimization stuck into a local minimum of the cost function without further improvement. The choice of γ_i using the Taguchi method may lead to a response with high-frequency oscillations in the system.

The next step of the proposed methodology is to apply the discrete cosine transform (DCT) technique to the Taguchi optimization process, consider the spectral content of the response to the cost function, and determine the optimal values of γ_i to avoid oscillations in the output of the system.

3 Problem Solution

3.1 Simulation Results

When the optimization is performed on the MRAC while the process lasts, the error does not converge to zero in a short time.

The MRAC attempts to minimize the error, but the Taguchi optimization continuously changes the parameters $\gamma_1, \gamma_2, \gamma_3,$ and γ_4 of the system. This results in the error continuously deviating from zero, occurring just in time when the Taguchi optimization changes the parameters γ_i .

In Fig.6, the optimization procedure is demonstrated, which exploits the initial time space where the error takes its maximum value and is described using markers. The error is depicted by a blue line, and the upper boundary of the error located at its peaks is indicated by a dashed red line. The green circles describe the points where the Taguchi optimization is activated and operates, that is, the combinations of each row of the orthogonal array. With red circles, the moment when all the experimental runs of the orthogonal array are completed, and the selection of the best parameters that minimize the Cost Function are made.

The calculation of the DCT and imposition of the penalty were performed at the points marked with black asterisks. The calculation of the DCT and finding the average of all peaks with a frequency greater than the first peak participates in the calculation of the Cost Function. It should be noted that the first peak is the fundamental frequency of the system's operation. This average for the highest frequencies imposes an increase in the Cost Function as a penalty that punishes the appearance of high frequencies in the system so that the parameters γ_i can be appropriately adjusted so that

rapid changes are not displayed in the system and the system's response becomes smoother.

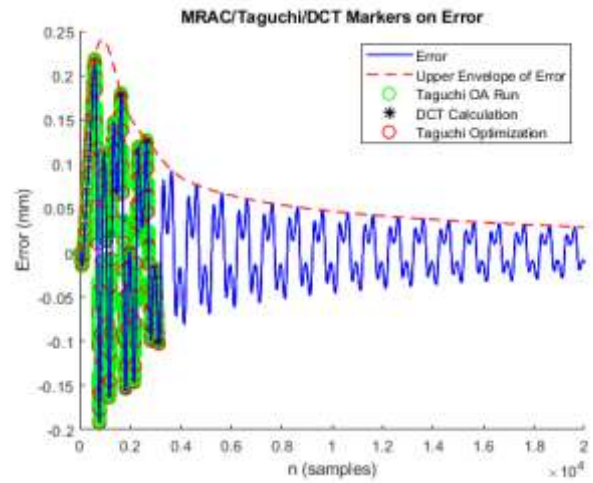


Fig. 6: The optimization procedure using Taguchi and DCT.

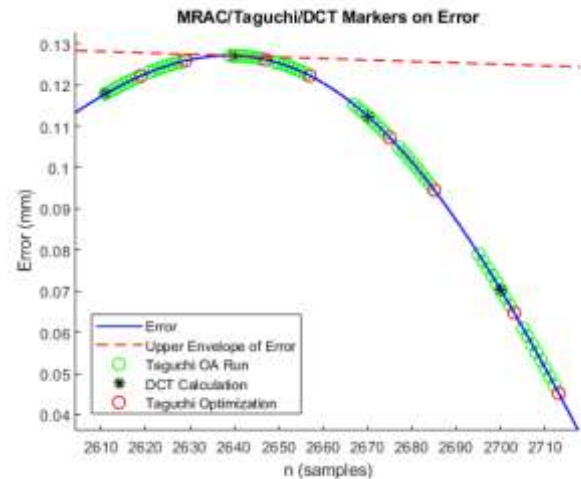


Fig. 7: A zoomed region of the optimization procedure using Taguchi and DCT.

In Fig.7, which is a small area in Fig.6. is presented, where the operating points of the system are clearly visible.

Taguchi-DCT optimization is performed in real time at the system startup to adjust the γ_i parameters. When the optimization objectives are achieved, the optimization algorithm is turned off, and the system is left free to operate only with MRAC to adapt the plant to the reference model.

In Fig.8 the comparative results of the proposed MRAC-Taguchi-DCT and simple MRAC methods are presented, when the constant parameter is $\gamma = -10$ and the frequency is 100 mHz.

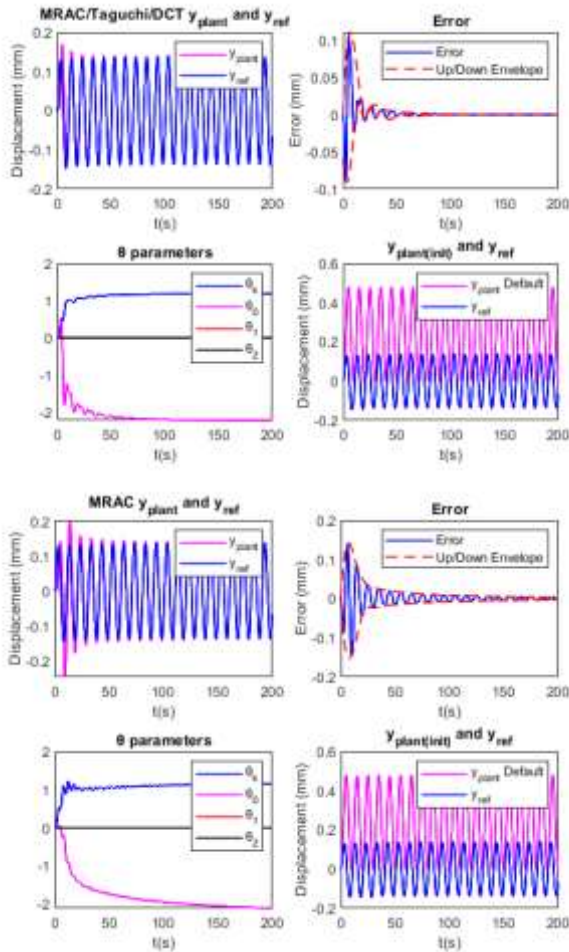


Fig. 8: Comparative results of the proposed MRAC-Taguchi-DCT and simple MRAC methods, $\gamma = -10$ and 100 mHz.

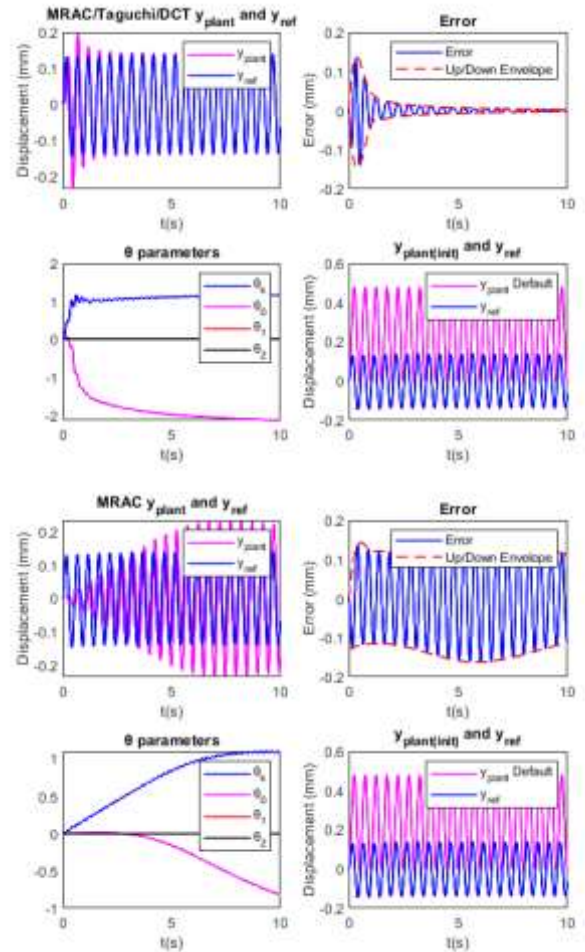


Fig. 9: Comparative results of the proposed MRAC-Taguchi-DCT and simple MRAC methods, $\gamma = -10$ and 2 Hz.

With the proposed optimization method, the error converges to zero faster and the θ parameters of the MRAC system converge and stabilize faster. In Fig.9, the comparison results with MRAC-Taguchi-DCT and simple MRAC for a frequency of 2 Hz are presented. In Fig.10 comparison results for 10 Hz are shown.

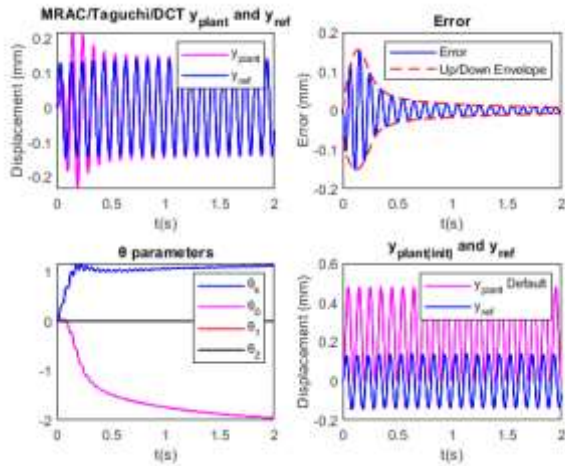


Fig. 10: Comparative results of proposed MRAC-Taguchi-DCT and simple MRAC methods, $\gamma = -10$ and 10 Hz.

In Fig.11, the results of the MRAC-Taguchi function without DCT optimization for a frequency of 10 Hz are presented. The significant presence of harmonic frequencies in the system is shown in Fig.12 in contrast with Fig.13 where DCT optimization is enabled and the harmonics have a smaller appearance in the spectrum. Furthermore, as shown in Fig.12, the amplitude of the fundamental frequency of the error is suppressed. In both graphs, the discrete Fourier transform (DFT) spectrum is presented with the FFT and DCT for comparison.

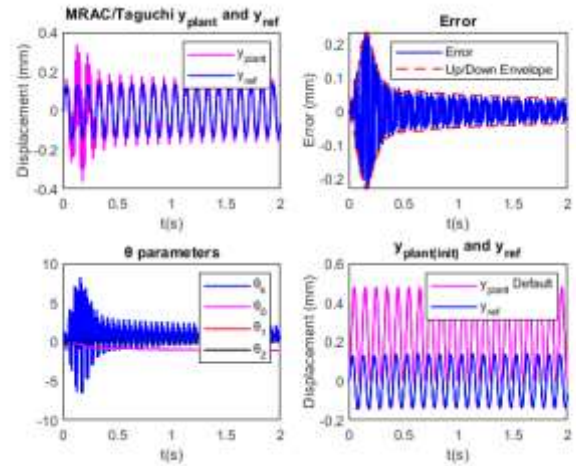


Fig. 11: The MRAC-Taguchi operation without DCT optimization at a frequency of 10 Hz.

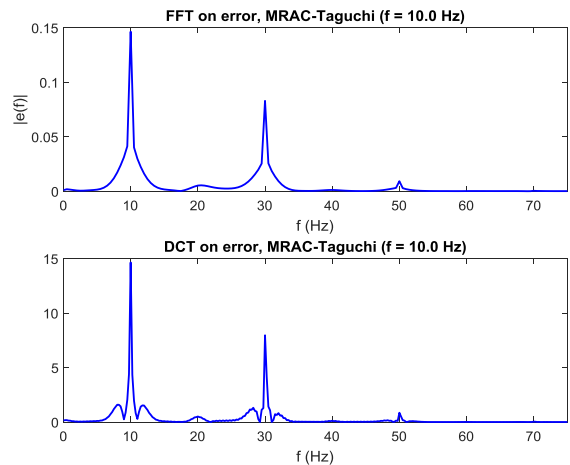
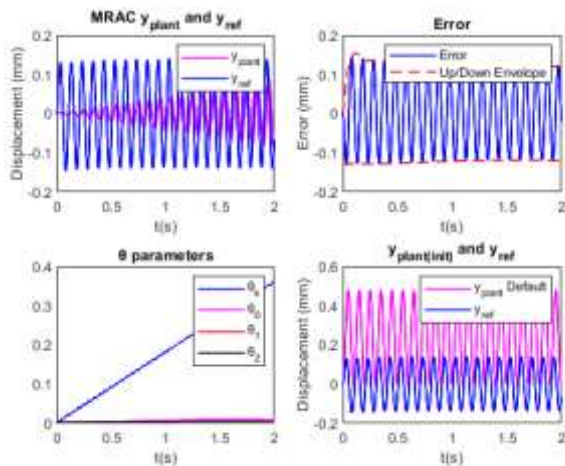


Fig. 12: Presence of other harmonic frequencies in the system without DCT optimization.

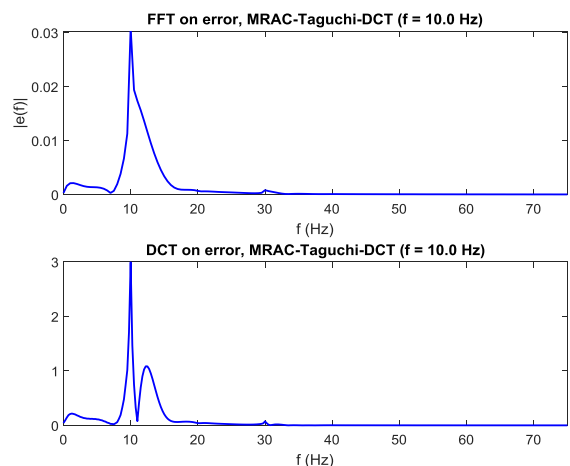


Fig. 13: The spectrum with DCT optimization.

The values of γ_i for all the operating frequencies presented in the graphs above are listed in Table 3.

Table 3. Values of γ_i for all operating frequencies of the tested methods.

Method	f (Hz)	$ \gamma_1 $	$ \gamma_2 $	$ \gamma_3 $	$ \gamma_4 $
MRAC	0.1/2/10	10	10	10	10
MRAC-Taguchi-DCT	0.1	10.31	85.93	9.45	8.59
MRAC-Taguchi-DCT	2	180.45	226.85	137.49	85.93
MRAC-Taguchi	10	53163	147.68	116.16	660.99
MRAC-Taguchi-DCT	10	498.39	523.31	88.51	119.44

In particular, for the case of 10 Hz, a large difference was observed in the values of the parameters between MRAC-Taguchi and MRAC-Taguchi-DCT.

3.2 Experimental Results

The results of the experimental setup are presented in Fig.A in Appendix. The reference signal that the IPMC should follow with its movement is shown at the top of the graph, followed by the response of the IPMC using only MRAC (with a fixed $\gamma = 10$), the response with MRAC-Taguchi, and finally the response with MRAC-Taguchi-DCT. The target is approached rapidly by the MRAC-Taguchi response, but the choices of γ made through the optimization do not consider the frequency content of the response, and the optimization can lock into a local minimum without further improving γ_i . In contrast, it is observed that with the MRAC-Taguchi-DCT technique, frequencies beyond the fundamental frequency are penalized through the Cost Function, and the result appears with negligible harmonic distortion, mainly due to low-amplitude frequencies adjacent to the fundamental frequency. Moreover, it appears that in the time interval from 0 to approximately 0.2 s, harmonic frequencies are present, and it is this time where the necessary number of samples is collected, in order for the DCT to output more accurately the coefficients that will penalize the presence of harmonic frequencies and will direct the optimization to better choices of γ_i , which can be seen by a rapid decrease in harmonic distortion after 0.2 s.

4 Conclusion

The MRAC technique is a control method that uses a reference model to control a plant with unknown dynamics. The controller continuously updates its parameters to improve control accuracy. However, parameter γ cannot have a fixed value and should be adjusted in real time with the rest of the system parameters and various exogenous factors. The proposed method uses real-time optimization techniques to optimize the parameters during system startup and whenever the error suddenly changes.

The MRAC-Taguchi-DCT optimization method has been proposed to improve the performance of MRAC (Model Reference Adaptive Control) system. This optimization technique continuously changes γ_i parameters of the MRAC system to minimize the error. The calculation of the DCT and imposition of the penalty were performed to ensure a smoother response of the system. The comparative results of the proposed MRAC-Taguchi-DCT method have been presented and show that the error converges to zero faster, and the θ parameters of the MRAC system converge and stabilize faster when compared to MRAC with one and constant parameter γ . Overall, the MRAC-Taguchi-DCT optimization method improved the performance of the MRAC system and achieved the fastest convergence and stabilization of the θ parameters. This leads to a more accurate control signal and reduces strain on the plant.

One possible future development of this work is the use of machine learning techniques, such as deep learning and reinforcement learning, to enhance the adaptive capabilities of the control system. These techniques have shown promising results in other applications, and there is potential for their application to MRAC control. These techniques can be implemented, compared, or integrated into the existing system, leading to more robust and adaptable control systems that can handle a wider range of uncertainties and disturbances.

References:

- [1] Jung, K., Nam, J. and Choi, H., 2003. *Investigations on actuation characteristics of IPMC artificial muscle actuator. Sensors and Actuators A: Physical*, 107(2), pp.183-192.
- [2] Bonomo, C., Fortuna, L., Giannone, P., Graziani, S. and Strazzeri, S., 2006. Motion sensors and actuators based on ionic polymer-metal composites. *Device Applications of Nonlinear Dynamics*, pp.83-99.

- [3] Bhandari, B., Lee, G.Y. and Ahn, S.H., (2012). A review on IPMC material as actuators and sensors: fabrications, characteristics and applications. *International journal of precision engineering and manufacturing*, 13, pp.141-163.
- [4] Lee, S.J., Han, M.J., Kim, S.J., Jho, J.Y., Lee, H.Y. and Kim, Y.H., 2006. A new fabrication method for IPMC actuators and application to artificial fingers. *Smart Materials and Structures*, 15(5), p.1217.
- [5] Yanamori, H., Kobayashi, T. and Omiya, M., 2011, January. Ionic polymer metal composite (IPMC) for MEMS actuator and sensor. *In International Electronic Packaging Technical Conference and Exhibition* (Vol. 44618, pp. 417-424).
- [6] Moeinkhah, H., Rezaeepazhand, J. and Akbarzadeh, A., 2013. Analytical dynamic modeling of a cantilever IPMC actuator based on a distributed electrical circuit. *Smart Materials and Structures*, 22(5), p.055033.
- [7] Vahabi, M., Mehdizadeh, E., Kabganian, M. and Barazandeh, F., 2011. Experimental identification of IPMC actuator parameters through incorporation of linear and nonlinear least squares methods. *Sensors and Actuators A: Physical*, 168(1), pp.140-148.
- [8] Liu, Y., Chang, L., Hu, Y., Niu, Q., Yu, L., Wang, Y., Lu, P. and Wu, Y., 2018. Rough interface in IPMC: modeling and its influence analysis. *Smart Materials and Structures*, 27(7), p.075055.
- [9] Aabloo, A., Belikov, J., Kaparin, V. and Kotta, Ü., 2020. Challenges and perspectives in control of ionic Polymer-Metal Composite (IPMC) Actuators: A Survey. *IEEE Access*, 8, pp.121059-121073.
- [10] Wang, J., McDaid, A., Sharma, R. and Aw, K.C., 2015, May. A compact ionic polymer metal composite (IPMC) system with inductive sensor for closed loop feedback. *In Actuators* (Vol. 4, No. 2, pp. 114-126).
- [11] Brufau-Penella, J., Tsiakmakis, K., Laopoulos, T. and Puig-Vidal, M., 2008. Model reference adaptive control for an ionic polymer metal composite in underwater applications. *Smart Materials and Structures*, 17(4), p.045020.
- [12] Yun, K. and Kim, W.J., 2006. System identification and microposition control of ionic polymer metal composite for three-finger gripper manipulation. *Proceedings of the Institution of Mechanical Engineers, Part I: Journal of Systems and Control Engineering*, 220(7), pp.539-551.
- [13] Nagpure, T. and Chen, Z., 2016. Control-oriented modeling of ionic polymer-metal composite enabled hydrogen gas production. *International Journal of Hydrogen Energy*, 41(16), pp.6619-6629.
- [14] Wang, J., McDaid, A., Sharma, R. and Aw, K.C., 2015, May. A compact ionic polymer metal composite (IPMC) system with inductive sensor for closed loop feedback. *In Actuators* (Vol. 4, No. 2, pp. 114-126).
- [15] Ekbatani, R.Z., Shao, K., Khawwaf, J., Wang, H., Zheng, J., Chen, X. and Nikzad, M., 2021, February. Control of an IPMC soft actuator using adaptive full-order recursive terminal sliding mode. *In Actuators* (Vol. 10, No. 2, p. 33).
- [16] Biswal, D.K., Moharana, B.R. and Mohapatra, T.P., 2022. Bending response optimization of an ionic polymer-metal composite actuator using orthogonal array method. *Materials Today: Proceedings*, 49, pp.1550-1555.
- [17] Park, J., Ham, J.W., Park, S., Kim, D.H., Park, S.J., Kang, H. and Park, S.O., 2017. Polyphase-basis discrete cosine transform for real-time measurement of heart rate with CW Doppler radar. *IEEE Transactions on Microwave Theory and Techniques*, 66(3), pp.1644-1659.
- [18] Karna, S.K. and Sahai, R., 2012. An overview on Taguchi method. *International journal of engineering and mathematical sciences*, 1(1), pp.1-7.

Contribution of Individual Authors to the Creation of a Scientific Article (Ghostwriting Policy)

Kyriakos Tsiakmakis, has implemented the algorithms and control system
Vasileios Delimaras, carried out the simulations and the optimization algorithms.
Argyrios Xatzopoulos, has organized the simulations and experiments
Maria Papadopoulou, has organized the simulations and experiments

Sources of Funding for Research Presented in a Scientific Article or Scientific Article Itself

No funding was received for conducting this study.

Conflict of Interest

The authors have no conflicts of interest to declare that are relevant to the content of this article.

Creative Commons Attribution License 4.0 (Attribution 4.0 International, CC BY 4.0)

This article is published under the terms of the Creative Commons Attribution License 4.0

https://creativecommons.org/licenses/by/4.0/deed.en_US

Appendix

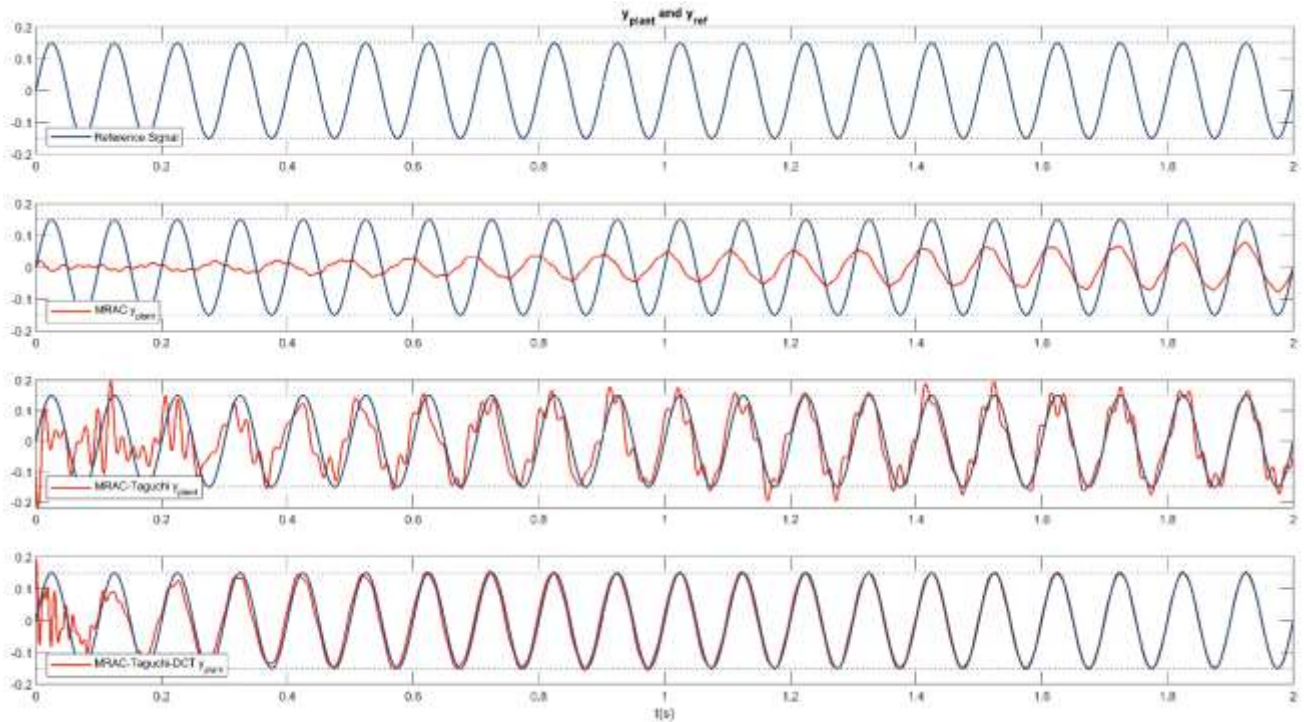


Fig. A: The reference signal (top and in all following graphs) and the responses of MRAC, MRAC-Taguchi, and MRAC-Taguchi-DCT, respectively.